Stiffness Tailoring for Improved Compressive Strength of Composite Plates with Holes

Raphael T. Haftka*
Virginia Polytechnic Institute and State University, Blacksburg, Virginia
and
James H. Starnes Jr.†
NASA Langley Research Center, Hampton, Virginia

A structural optimization procedure is used to obtain minimum-mass designs of compression-loaded composite plates with holes by tailoring the plate cross-sectional stiffnesses. The plate cross sections consist of two different balanced symmetric laminates with 0, ±45, and 90 deg plies. The plate inner laminate contains a hole and is designed from a softer material system with a higher failure strain than the plate outer laminate. All-graphite-epoxy plates and hybrid graphite/glass-epoxy plates were studied. Results for designs with different percentages of 0 and ±45 deg plies in the outer laminate are compared with results for the optimum designs. Results for designs with uniform cross-sectional stiffnesses are also compared with the results for tailored cross-sectional stiffness designs. Specimens of each design were tested to verify the analytical predictions. The results show that cross-sectional stiffness tailoring can increase the ratio of compressive strength to mass of compression-loaded laminated plates with holes. It is shown that removing 0 deg plies from the hole region both increases the compression strength and decreases the mass of graphite-epoxy plates.

Introduction

THE problem of strength reduction of plates due to holes has been studied for many years. Recently, optimization methods have been used to minimize the adverse effects of a hole without incurring large mass penalties. One approach is to modify the hole shape to minimize the stress concentrations (Ref. 1). Another approach is to reinforce the region near the hole to minimize the stress concentrations (Ref. 2). Because changing the hole shape is often not practical, hole reinforcement has been the treatment of choice by most designers.

The problem of stress concentrations due to holes and their effect on failure loads is more severe for composite plates than for metal ones. Composite materials tend to be more brittle than metals and, therefore, provide little or no relief due to plastic load redistribution. In addition, load is transferred from the plate to the hole reinforcement through a soft, weak resin layer. This load transfer can cause shear-lag and shear-failure problems in the reinforced region unless special measures, such as bolts or stitching through the laminate thickness, are used.

An alternative to hole reinforcement is to use a softer material that can withstand high strains in the hole region. It is shown analytically in Ref. 3 that replacing the high-modulus 0 deg graphite fibers near a hole with low-modulus, high-failure-strain 0 deg glass fibers can increase the failure load of a tension-loaded composite plate. The results presented in Ref. 3 suggest that tailoring the cross-sectional stiffness distribution of a laminated plate by softening the laminate near a hole also may increase the compressive strength of the plate. It is shown in Ref. 4 that ±45 deg fiber-dominated graphite-epoxy laminates are softer and have higher failure strains than 0 deg fiber-dominated graphite-epoxy laminates. These results suggest that the use of a ±45 deg fiber-dominated graphite-epoxy laminate near a hole may achieve the same effect as the use of glass fibers near the hole.

Failure of compression-loaded composite plates with holes is studied in several recent publications (Refs. 5 and 6). It is shown in Ref. 6 that failure of compression-loaded 0 deg fiber-dominated graphite-epoxy plates with holes can be predicted by the point-stress failure criterion of Ref. 7. The present paper presents the results of a study of the use of cross-sectional stiffness tailoring to improve the compressive strength of composite plates with holes. The criterion of Ref. 7 is used to predict failure. The WIDOWAC program[8] is used to analyze the composite plates and to obtain minimum-mass designs that were fabricated and tested. These minimum-mass designs are used as reference-point designs for several studies that demonstrate the effectiveness of cross-sectional stiffness tailoring to improve the compressive strength of composite plates with holes. Analytical failure predictions for all plates are compared with experimental results.

Analysis and Optimization

The WIDOWAC program[8] used in this study for the analysis and optimization of the composite plates employs membrane quadrilateral finite elements composed of four triangular elements. Because of the symmetry of the problem, only one quarter of the plate was modeled, and each ply orientation was modeled by a separate finite element. The panel geometry is shown in Fig. 1, and a typical finite-element model is shown in Fig. 2 with each element representing several elements stacked on top of one other.

The results of the finite-element analysis are used to predict failure by employing a modified Whitney-Nuismer

Presented as Paper 85-0721 at the AIAA/ASME/ASCE/AHS 26th Structures, Structural Dynamics and Materials Conference, Orlando, FL, April 15–17, 1985; received Sept. 3, 1986; revision received May 22, 1987.

*Professor, Department of Aerospace and Ocean Engineering. Member AIAA.

†Head, Structural Mechanics Branch, Structures and Dynamics Division, Associate Fellow AIAA.

point-stress failure criterion.[7] The point-stress failure criterion is based on the premise that failure occurs when stress at a small characteristic dimension d away from the hole edge reaches the ultimate strength of the material. The point-stress criterion is modified herein to a point-strain criterion applied to the principal load-carrying plies of the laminate. The characteristic dimension d and the ultimate-strain values used for the graphite-epoxy in this study are based on data from Refs. 4 and 6.

The optimization algorithm employed by WIDOWAC is the quadratic extended interior penalty function method.[9] Unconstrained minimizations are performed by Newton's method with approximate second derivatives. The plates were optimized to achieve minimum mass subject to a constraint that the strain in any element does not exceed its critical value. The point-strain criterion approach was implemented by not applying the constraint to the first row of elements near the hole.

The design load is 444 kN of axial compression plus 44 kN of lateral compression to insure that the design can carry some lateral load. The design variables are the thicknesses of the 0, 90, and ±45 deg plies (the thicknesses of the +45 and −45 deg plies are the same to insure symmetry) in two regions of the plate—an inner region containing the hole and an outer region. Compression-loaded plates with high percentages of 0 deg plies have complex and, sometimes, unpredictable failure modes. To protect against these failure modes, an upper limit of 50% of the total number of plies was imposed on the amount of 0 deg plies (a conservative limit based on the data available when the plates were designed). The ±45 deg and 90 deg plies were required to be continuous over the entire specimen and minimum gage constraints were also imposed. The ply thicknesses were treated as continuous design variables, with the optimum thicknesses rounded up to an integer number of plies.

Specimens, Apparatus and Tests

Both all-graphite-epoxy specimens and hybrid specimens made of graphite-epoxy and glass-epoxy materials were tested in this investigation. The all-graphite-epoxy specimens were made from commercially available 0.13-mm-thick unidirectional Hercules AS-4 graphite-fiber tapes preimpregnated with 450K cure Hercules 3502 thermosetting epoxy resin. The hybrid graphite/glass-epoxy specimens were made from Hercules AS4/3502 graphite-epoxy tapes and from 0.16-mm-thick S-2 glass fiber tapes that were also preimpregnated with Hercules 3502 epoxy resin. The tapes were laid up to form laminated plates with balanced, symmetric laminates consisting of 0, 90, and ±45 deg plies. The cross section of some of the plates consisted of two different laminates (the inner and outer laminates in Fig. 1). The inner laminate was made to have lower longitudinal stiffness and higher failure strain than the outer laminate. The other plates consisted of the stiffer outer laminate only. Plates with two different laminates are referred to herein as the tailored-stiffness designs, and plates with only one laminate are referred to as the uniform-stiffness designs.

In most cases the tailored-stiffness designs had outer laminates that were thicker than the inner laminates causing a thickness discontinuity at the boundary. For some specimens all ±45 and 90 deg fibers were continuous across the specimen; for other specimens some of the outer ±45 deg fibers were terminated at the discontinuity and not continued into the inner laminate. In some cases 90 deg fibers were added to the inner laminate to provide a uniform thickness even though these designs still had discontinuous stiffnesses.

The laminated plates were cured in an autoclave using the resin manufacturer's recommended procedure. Following cure, the laminates were ultrasonically inspected and only laminates without detectable flaws were tested. Extensive data for the graphite-epoxy material system are available. Typical lamina properties for the cured plies are 131.0 GPa for the longitudinal Young's modulus E_1, 13.0 GPa for the transverse Young's modulus E_2, 6.4 GPa for the shear modulus G_{12}, and 0.38 for the major Poisson's ratio ν_{12}. The characteristic dimension d for the point-strain failure criterion was taken to be 0.05 cm, and the ultimate-strain values used are 0.014 for the 0 deg plies and 0.024 for the ±45 plies. To determine the properties of the glass-epoxy system, tests were performed on three unnotched panels with

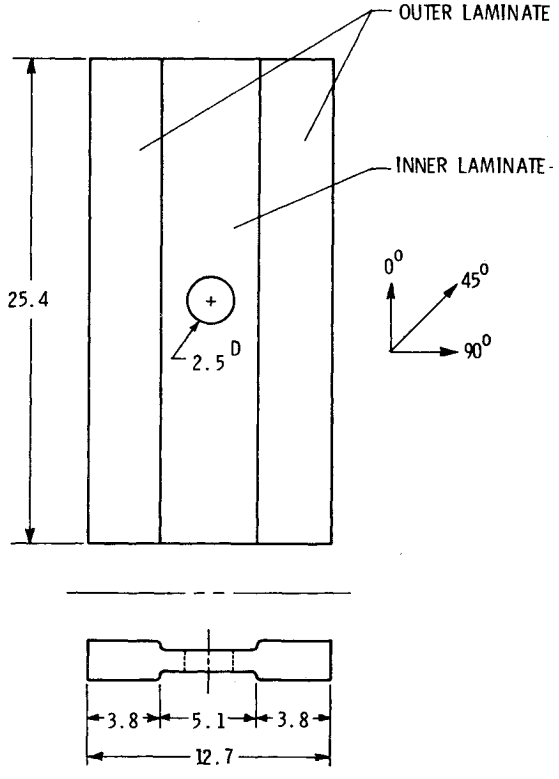

Fig.1 Tailored-stiffness plate geometry (dimensions are in cm).

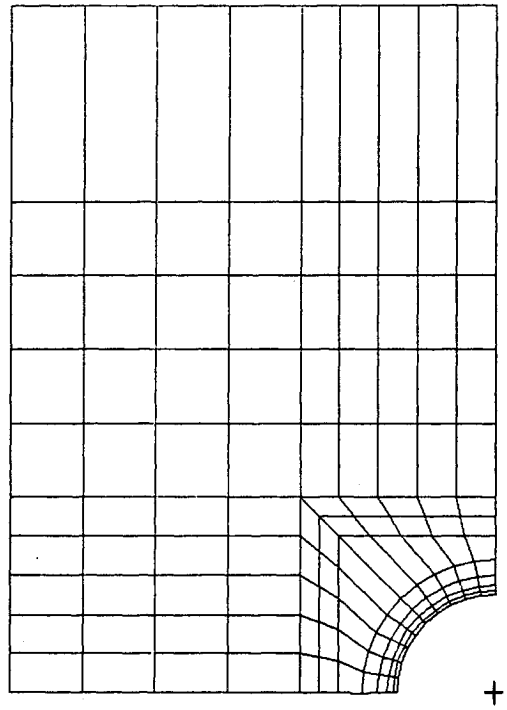

Fig. 2 One-quarter plate finite-element model.

various combinations of 0, 90, and ±45 deg plies. The unidirectional properties were then determined by a least-squares curve fit of measured longitudinal moduli and Poisson's ratios for the three laminates. The resulting lamina properties for the cured glass-epoxy plies are 50.8 GPa for E_1, 11.4 GPa for E_2, 6.45 GPa for G_{12}, and 0.415 for ν_{12}. Test results for notched plates suggested a value of d equal to 0.05 cm and ultimate-strain values of 0.024 for 0 deg dominated plates and 0.032 for ±45 deg dominated plates.

The specimens were 25.4 cm long and 12.7 cm wide and most had a 2.5-cm-diam hole in the center of the specimens as shown in Fig. 1. The holes were machined into the specimens with a diamond-impregnated core drill. The ends of the specimens were ground flat and parallel to permit uniform compressive loading.

The specimens were loaded in axial compression using a 1.33-MN-capacity hydraulic testing machine. The loaded ends of the specimens were clamped by fixtures during testing, and the unloaded edges were simply supported by knife-edge restraints to prevent the specimens from buckling as wide columns. A typical specimen in the support fixture is shown in Fig. 3. Twenty-five all-graphite-epoxy, eight hybrid graphite/glass-epoxy, and one all-glass-epoxy specimens were tested to failure in static compression.

Electrical resistance strain gages were used to monitor strains and direct-current differential transformers were used to monitor displacements at selected locations on the specimens. All electrical signals and the corresponding applied loads were recorded on magnetic tape at regular time intervals during the tests.

Results and Discussion

The optimal designs were obtained analytically for the geometry of Fig. 1. The optimization procedure always produced designs which had a minimum gage of 90 deg plies, and the maximum amount of 0 deg plies in the outer laminate. Design studies for nonoptimal plates were performed by changing the laminate composition and the width of the softer inner laminate.

Optimum All-Graphite-Epoxy Design

The results for the optimum all-graphite-epoxy design, and for nonoptimal all-graphite-epoxy designs are presented in Table 1. The optimum all-graphite-epoxy design was predicted to fail at an applied load of 523 kN and specimen G1, based on this design, failed at an applied load of 534 kN. The far-field membrane strain at failure was 0.0088 in the stiffer outer laminate and 0.0093 in the softer inner laminate with the hole. The stiffnesses of both laminates decreased slightly as the load increased indicating some material nonlinearity. The membrane strain near the hole (approximately 0.076 cm from the hole edge) at failure was 0.0194. Failure of specimen G1 occurred away from the hole.

The uniform-stiffness design based on the stiffer outer laminate of the optimum all-graphite-epoxy design was predicted to fail at an applied load of 491 kN, and specimen G1U, based on this design, failed at an applied load of 484 kN. The far-field membrane strain at failure was 0.0050 and the membrane strain near the hole at failure was 0.0146. Failure of specimen G1U occurred at the hole. These results indicate that the optimum all-graphite-epoxy tailored-stiffness design failed at a load that is 10% greater than the cor-

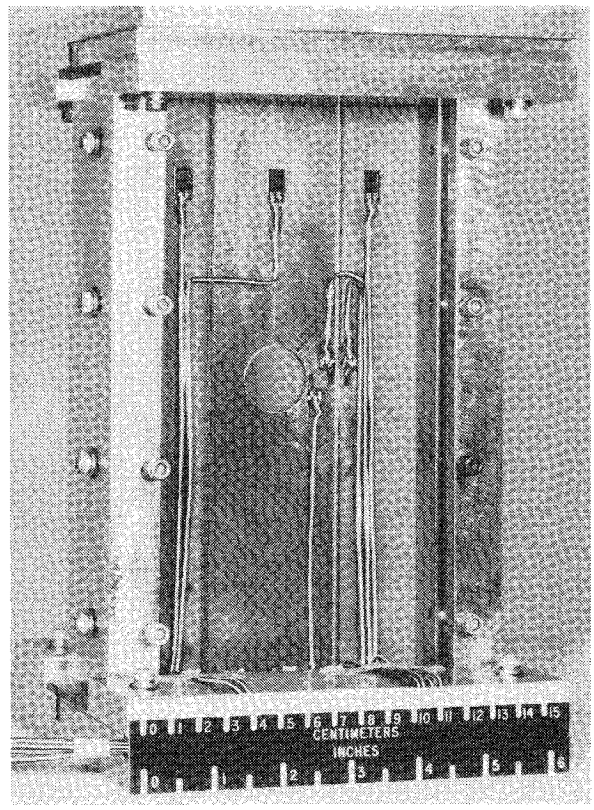

Fig. 3 Test specimen and support fixture.

Table 1 Effect of ply composition on failure loads of all-graphite-epoxy plates (all specimens have geometry shown in Fig. 1)

Specimen	Outer laminate	Inner laminate	Failure load, kN		Mass, kg
			Analysis	Test	
G1	$(0_{36}/45_{36}/90_6)$[a]	$(45_{36}/90_6)$	523	534	0.44
G1U	$(0_{36}/45_{36}/90_6)$	—	491	484	0.55
G2	$(0_{24}/45_{48}/90_6)$	$(45_{36}/90_6)$	419	450	0.44
G2U	$(0_{24}/45_{48}/90_6)$	—	381	428	0.53
G3	$(0_{24}/45_{48}/90_6)$	$(45_{48}/90_6)$	432	481	0.44
G3U	$(0_{24}/45_{48}/90_6)$	—	381	410	0.50
G4	$(0_{12}/45_{60}/90_6)$	$(45_{36}/90_6)$	316	334	0.44
G4U	$(0_{12}/45_{60}/90_6)$	—	268	289	0.54
G5	$(0_{12}/45_{60}/90_6)$	$(45_{60}/90_6)$	354	404	0.49
G5U	$(0_{12}/45_{60}/90_6)$	—	268	333	0.52
G6	$(45_{72}/90_6)$	$(45_{36}/90_6)$	214	231	0.44
G6U	$(45_{72}/90_6)$	—	262	275	0.51
G7	$(0_{48}/45_{24}/90_6)$	$(45_{24}/90_6)$	590	569	0.37
G7U	$(0_{48}/45_{24}/90_6)$	—	605	577	0.49
G8	$(0_{60}/45_{12}/90_6)$	$(45_{12}/90_6)$	655	557	0.35
G8U	$(0_{60}/45_{12}/90_6)$	—	699	671	0.49

[a] The laminate notation indicates the number of 0, ±45, and 90 deg plies in the laminate, not the stacking sequence.

Table 2 Laminates, failure loads and masses for hybrid graphite/glass-epoxy designs

Specimen	Outer laminate	Inner laminate	Failure load, kN		Mass, kg
			Analysis	Test	
H1	$(0_{24_{Gr}}/45_{20_{G1}}/90_{4_{G1}})^a$	$(0_{20}/45_{20}/90_4)_{G1}$	437	400	0.39
H1U	$(0_{24_{Gr}}/45_{20_{G1}}/90_{4_{G1}})$	—	316	309	0.38
H1G	$(0_{20}/45_{20}/90_4)_{G1}$	—	262	244	0.46
H2	$(0_{24_{Gr}}/45_{20_{G1}}/90_{4_{G1}})$	$(0_6/45_{20}/90_4)_{G1}$	372	390	0.36
H2U	$(0_{24_{Gr}}/45_{20_{G1}}/90_{4_{G1}})$	—	316	315	0.40
H3	$(0_{24_{Gr}}/45_{20_{G1}}/90_{4_{G1}})$	$(0_6/45_{20}/90_4)_{G1}$	372	377	0.39
H3U	$(0_{24_{Gr}}/45_{20_{G1}}/90_{4_{G1}})$	—	316	306	0.44
H4	$(0_{28}/45_{28}/90_6)_{Gr}$	$(0_{8_{G1}}/45_{28_{Gr}}/90_{6_{Gr}})$	453	386	0.37
H4U	$(0_{28}/45_{28}/90_6)_{Gr}$	—	384	373	0.41
H5	$(0_{24}/45_{24}/90_4)_{Gr}$	$(0_{20_{G1}}/45_{24_{Gr}}/90_{4_{Gr}})$	441	406	0.37
H5U	$(0_{24}/45_{20}/90_4)_{Gr}$	—	327	352	0.35

[a]The laminate notation indicates the number of 0 deg, ±45 deg, and 90 deg plies in the laminate, not the stacking sequence.

responding uniform-stiffness design and has a 20% lower mass.

Modified All-Graphite-Epoxy Designs

Modified all-graphite-epoxy designs were also studied to determine the effect of stiffness distribution on ultimate loads. The effect of varying the relative percentage of 0 and ±45 deg plies was investigated, and the results are summarized in Table 1. Specimens G2, G3, G4, G5, and G6 have fewer 0 deg plies and more ±45 deg plies than the optimum design. The ±45 deg plies are continuous across specimens G3 and G5 so that the thicknesses of the inner laminates change from specimen to specimen. Specimens G2, G4, and G6 maintain the same thickness for both inner and outer laminates as the optimum design. As a result, some of the ±45 deg fibers are present only in the outer laminates.

Specimens G7 and G8 have more 0 deg plies than the optimum design. They violate the requirement imposed on the optimum design that the maximum number of 0 deg plies not exceed the upper limit of 50% of the total number of plies. Consequently, ultimate compressive loads for these specimens are higher than for the optimal design.

The effect of varying the percentage of 0 deg plies is shown graphically in Fig. 4. The failure load of each design in Table 1 is normalized by the specimen mass so that designs can be compared on a strength-to-mass basis. The squares and circles of Fig. 4 represent the tailored-stiffness and uniform-stiffness design test data, respectively, and the solid and dashed lines represent the corresponding analytical predictions. The double values of the results for some percentages of 0 deg plies represent the differences in specimens with continuous and discontinuous ±45 deg plies between the inner and outer laminates of the specimens. The maximum gain in strength of the tailored stiffness specimens is 21% for specimen G5 (15% 0 deg plies). For very high percentages of 0 deg plies, the effect of removing 0 deg plies from the hole region on the total stiffness outweighs the increased failure strain near the hole. Therefore, the uniform-stiffness specimens with very high percentages of 0 deg plies are stronger than the corresponding tailored-stiffness specimens.

The agreement between the analysis and experiment is surprisingly good considering that failure predictions are based on a fairly coarse mesh of low-order finite elements and a simple failure criterion. The average difference between the analytical and experimental results for the all-graphite-epoxy plates is about 8%. There are only two specimens (out of 16) where the difference between analysis and experiments is

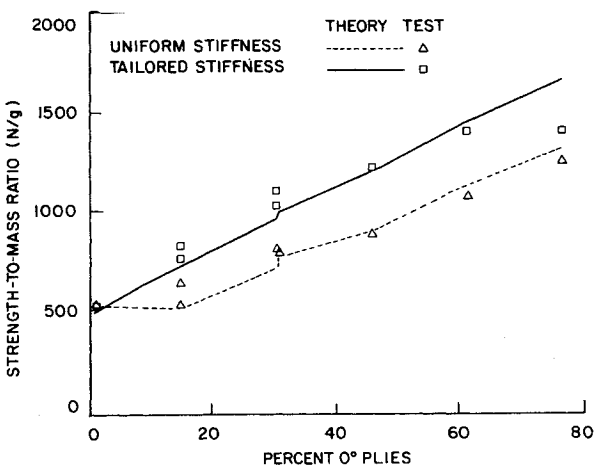

Fig. 4 Failure strength-to-mass ratio for all-graphite-epoxy plates.

substantial. For specimen G8, the inner laminate is so thin that the failure was probably due to buckling that was not modeled analytically. For specimen G5U, the large difference between analysis and test is inconsistent with the results for specimen G4U, which is identical in composition to specimen G5U but failed at a 13% lower load than specimen G5U and much closer to the analytical prediction. This difference of 13% between specimens G4U and G5U is high for the cases where tests were repeated with specimens of identical specifications. The other identical specimens, i.e., specimens G2U and G3U, have failure loads that were within about 4% of each other.

Hybrid Graphite/Glass-Epoxy Designs

Two types of hybrid graphite/glass-epoxy designs were considered. The first type consisted of a glass-epoxy laminate with the 0 deg glass fibers replaced by 0 deg graphite fibers in the outer laminate. The second type was a graphite-epoxy laminate with the 0 deg fibers near the hole replaced by glass fibers. The first type is referred to herein as a graphite-reinforced glass-epoxy laminate, and the second is referred to as a glass-softened graphite-epoxy laminate.

Specimen H1 in Table 2 is a graphite-reinforced glass-epoxy specimen designed by the optimization procedure. Two uniform-stiffness specimens were tested for comparison. Specimen H1U corresponds to the outer laminate of

Table 3 Effect of inner laminate width on graphite-epoxy laminates with 2.5 cm hole

Outer laminate	Inner[b] laminate width, cm	Failure load, kN		Normalized strength-to-mass ratio[c]
		Analysis	Test	
$(0_{36}/45_{36}/90_6)$[a]	6.4	461	500	1.33
	5.1	523	531	1.33
	3.8	640	—	—
	3.2	782	646	1.46
	0.0	491	485	1.00
$(0_{24}/45_{48}/90_6)$	5.1	419	449	1.28
	3.8	503	496	1.34
	3.2	601	503	1.34
	0.0	381	428	1.00

[a]The laminate notation indicates the number of 0 deg, ±45 deg, and 90 deg plies in the laminate, not the stacking sequence. [b]The inner laminate consists of $(45_{36}/90_6)$ plies. [c]Test results of strength-to-mass ratio of variable stiffness specimen normalized by strength-to-mass ratio of uniform-stiffness specimen.

Table 4 Effect of adding 90 deg plies to inner laminate to obtain constant-thickness graphite-epoxy laminates

Specimen	Outer laminate	Inner laminate	Failure laod, kN test
G1	$(0_{36}/45_{36}/90_6)$[a]	$(45_{36}/90_6)$	534
G1U	$(0_{36}/45_{36}/90_6)$	—	484
G1N	$(0_{36}/45_{36}/90_6)$	$(45_{36}/90_{42})$	527
G3	$(0_{24}/45_{48}/90_6)$	$(45_{48}/90_6)$	481
G3U	$(0_{24}/45_{48}/90_6)$	—	410
G3N	$(0_{24}/45_{48}/90_6)$	$(45_{48}/90_{30})$	429
G5	$(0_{12}/45_{60}/90_6)$	$(45_{60}/90_6)$	404
G5U	$(0_{12}/45_{60}/90_6)$	—	333
G5N	$(0_{12}/45_{60}/90_6)$	$(45_{60}/90_{18})$	332

[a]The laminate notation indicates the number of 0 deg, ±45 deg, and 90 deg plies in the laminate, not the stacking sequence.

specimen H1, and specimen H1G is an all-glass-epoxy laminate corresponding to the inner laminate of specimen H1. Comparing the results for specimens H1, H1U, and H1G, indicates that replacing the 0 deg glass plies by 0 deg graphite plies throughout the laminate increases the failure load by 27%, while selectively replacing only the outer-laminate 0 deg fibers increases the failure load by 64%.

Two other graphite-reinforced glass-epoxy specimens, H2 and H3, were designed earlier on the basis of different material properties and the experiment was repeated to assess scatter. The two plates were intended to be identical. Specimens H2 and H3 are a few percent weaker than the optimum design H1, but like specimen H1 they are substantially stronger than the corresponding uniform-stiffness plates H2U and H3U (24% and 23%, respectively). The agreement between analytical and experimental results is good with differences of 9% or less.

Some indication of experimental scatter is obtained by comparing the results for specimens H2 and H3 and for specimens H1U, H2U, and H3U that have identical compositions. Mass differences of 8% in the first group and 10% in the second group of specimens indicate manufacturing differences. The differences in failure loads are about 3% for both groups, and this small difference may indicate that the mass differences are mostly due to resin content.

The second type of hybrid, the glass-softened graphite-epoxy laminate, was optimized to produce the specimen H4 design. Another design of the same type, specimen H5, was optimized with the requirement of no thickness discontinuity. Like the other hybrid specimens, specimens H4 and H5 had lower failure loads than the predicted analytical loads (15% and 8%, respectively). Also, the improvements in failure loads over the uniform all-graphite specimens H4U and H5U are modest, and the gains in strength-to-mass ratios are 15 and 9%, respectively. It appears that a graphite panel benefits more from removing 0 deg plies near the hole than from replacing them with glass-epoxy plies.

Effect of Width of Inner Laminate

An inner laminate width of 5.1 cm was chosen initially in an attempt to remove the 0 deg graphite-epoxy plies from the regions of severe stress gradients near the 2.5 cm hole. However, the finite-element analysis predicted that much narrower inner laminates could be used. Table 3 shows the effect of inner-laminate width for two of the graphite-epoxy laminates of Table 1. In both cases the inner laminate is the outer laminate without the 0 deg plies. The design efficiency is presented in Table 3 as a strength-to-mass ratio normalized by the value of that ratio for the uniform-stiffness design.

The analytical predictions in Table 3 suggest that the inner-laminate width can be reduced to 3.2 cm and possibly even narrower. The experimental results indicate very little gain in strength by reducing the inner-laminate width from 3.8 cm to 3.2 cm. Also, the difference between the analytical and experimental failure loads for an inner-laminate width of 3.2 cm indicates that the coarse finite-element model and simple failure criterion are not adequate for modeling a thickness discontinuity so close to the hole boundary.

Thickness Discontinuity

One advantage of the hybrid designs is that they are easy to modify to obtain constant thickness designs (specimen H5 in Table 2). To achieve uniform thickness for the graphite-epoxy designs, soft 90 deg plies were added to the inner laminate. The results for three modified-graphite-epoxy-design specimens (specimens G1N, G3N, and G5N) are presented in Table 4 along with the corresponding specimens from Table 1. The results indicate that this design approach does not provide any benefit since the modified-design

constant-thickness specimens G1N, G3N, and G5N are weaker and heavier than specimens G1, G3, and G5.

Concluding Remarks

A structural optimization procedure was used to tailor the cross-sectional stiffness distribution of compression-loaded composite plates with holes. Minimum-mass designs were obtained for plates with cross sections consisting of two different balanced symmetric laminates with 0, ±45, and 90 deg plies. The plate inner laminate that contains a hole was designed from a softer material system with a higher failure strain than the material system used for the plate outer laminate. All-graphite-epoxy plates and hybrid graphite/glass-epoxy plates were studied. Other designs with different percentages of 0 and ±45 deg plies in the outer laminate were compared with the optimum designs. Designs with uniform cross-sectional stiffnesses corresponding to the outer laminate of the tailored-stiffness plates were used to demonstrate the improvements in compressive strength provided by the tailored-stiffness design approach. The analytical predictions based on a linear finite-element model and a point-strain failure criterion were validated by experiments.

In all cases the tailored-stiffness designs exhibited higher strength-to-mass ratios than the heavier uniform-stiffness designs. The improvement in the strength-to-mass ratio was highest for the hybrid designs of glass-epoxy panels reinforced by 0 deg graphite-epoxy plies in the outer laminate. Substantial improvements were also obtained for all-graphite-epoxy plates by removing the 0 deg plies from the inner laminate. Only modest gains were obtained by replacing 0 deg plies in all-graphite-epoxy plates with glass-epoxy plies in the inner laminate. The agreement between the experiments and analytical predictions was good, especially for the all-graphite-epoxy designs.

Acknowledgment

This research was supported in part by NASA Grant NAG-1-168.

References

[1]Dhir, S. D., "Optimization of Openings in Plates under Plane Stress," *AIAA Journal*, Vol. 21, Oct. 1983, pp. 1444–1448.

[2]Mansfield, E. J., "Neutral Holes in Plane Sheet-Reinforced Holes which are Elastically Equivalent to the Uncut Sheet," *Quarterly Journal of Mechanics and Applied Mathematics*, London, England, Vol. VI, Pt. 3, 1953, pp. 370–378.

[3]Sun, C. T. and Voit, P. M., "Improvement of the First-Ply-Failure Strength in Laminates by Using Softening Strips," *Composite Technology Review*, Vol. 3, No. 3, 1981, pp. 109–113.

[4]Shuart, M. J. and Williams, J. G., "Compression Failure Characteristics of ±45°-Dominated Laminates with a Circular Hole or Impact Damage," *AIAA Journal*, Vol. 24, Jan. 1986, pp. 115–122.

[5]Starnes, J. H. Jr., Rhodes, M. D., and Williams, J. G., "Effect of Impact Damage and Holes on the Compressive Strength of a Graphite/Epoxy Laminate," ASTM STP-696, 1979, pp. 145–171.

[6]Rhodes, M. D., Mikulas, M. M. Jr., and McGowan, P. E., "Effects of Orthotropy and Width on the Compression Strength of Graphite-Epoxy Panels with Holes," *AIAA Journal*, Vol. 22, Sept. 1984, pp. 1283–1292.

[7]Whitney, J. M. and Nuismer, R. J., "Stress Fracture Criteria for Laminated Composites Containing Stress Concentrations," *Journal of Composite Materials*, Vol. 8, 1974, pp. 253–265.

[8]Haftka, R. T. and Starnes, J. H. Jr., "WIDOWAC (Wing Design Optimization with Aeroelastic Constraints)," *Program Manual*, TM X-3071, NASA, 1974.

[9]Haftka, R. T. and Starnes, J. H. Jr., "Applications of a Quadratic Extended Interior Penalty Function for Structural Optimization," *AIAA Journal*, Vol. 14, June 1976, pp. 718–724.